ELSEVIER

Journal of Nuclear Materials 258–263 (1998) 927–933

journal of nuclear materials

The effective secondary electron yield in the space-charge limited condition

I.V. Tsvetkov [1], T. Tanabe *

Center for Integrated Research in Science and Engineering, Nagoya University, Furo-cho, Chikusa-ku, Nagoya 464-8603, Japan

Abstract

The dependence of the effective secondary electron yield on the potential distribution and the target materials was investigated by means of electron transport simulation in the sheath with the potential distribution calculated for the different emission characteristics of Be ($Z=4$), C ($Z=6$), Mo ($Z=42$) and W ($Z=74$) as the target materials. For lower primary energy incidence the effective secondary electron yield in the space-charge limited condition (SCLC) is markedly suppressed due to the prompt return of the secondary electrons. For higher energy electrons, the yield is independent of the potential distribution in the sheath and the energy distribution of the emitted electrons is shifted to higher energy direction. This effect would increase the sheath potential resulting in the increase of both ion energy flux to the surface and sputtering yield. Because of their high reflection coefficients this result should be very important for high Z materials but not for low Z materials.

1. Introduction

High Z materials, such as Mo and W, are important candidates for plasma facing materials in future fusion reactors because of their excellent thermophysical properties [1]. Quite recently detailed examinations of high Z behavior in plasma have been performed [2]. However, they mostly focus on the behavior of high Z impurities in the plasma and material performance under high heat loads. Under plasma exposure not only particle emission (including recycling hydrogen and sputtered particles) but also electron emission from the plasma facing materials should influence the boundary plasma. Until now, however, the effect of such electron emission, including both reflection and secondary electron emission, has not been examined well.

Basically high secondary electron yield is expected to reduce the sheath potential, which in turn suppresses the energy flux from the impact of plasma ions and reduces the sputtering yield and impurity production. On the other hand, prompt return of some part of the secondary electrons due to their gyromotion in an oblique magnetic field near the surface would reduce the effective electron emission yield. Also it should be noted that when a large amount of secondary electrons is emitted, a virtual cathode is formed just in front of the surface to weaken the electric field. In this respect, the formation of a hot spot on a divertor plate, where significant thermoelectron emission is expected, must be modified by the effective secondary yield or vice versa. This effect is important in case of high-Z materials, which have high secondary electron yield.

In the present work we have investigated how the effective electron emission yield is varied depending on the potential distribution and the target materials by means of 3-D electron transport simulation in the sheath taking into account of oblique magnetic field and the occurrence of the space charge limited condition. As for a target material, Be ($Z=4$), C ($Z=6$), Mo ($Z=42$) and W ($Z=74$) are selected and Z number effect is discussed.

2. Occurrence of the space-charge limited condition

As a first approximation, the potential distribution in the sheath was determined by solving Poisson's equation

* Corresponding author. Tel.: +81 52 789 5177; fax: +81 52 789 3791; e-mail: tanabe@cirse.nagoya-u.ac.jp.

[1] Permanent address: Moscow Engineering Physics Institute, 115409 Moscow, Russian Federation.

PII: S 0 0 2 2 - 3 1 1 5 (9 8) 0 0 3 1 2 - 2

assuming the ion temperature to be much lower than the electron temperature T_e and neglecting collision effects. Taking into account the suppression of emitted electrons from a plasma-facing materials by oblique magnetic field, we can modify the equation given by Hobbs and Wesson [3] as

$$\frac{d^2\chi}{d\xi^2} = -\frac{1}{\sqrt{1-\frac{\chi}{\varepsilon_i}}} + \left(1 - \frac{\gamma}{1-\gamma}\sqrt{-\frac{m_e\varepsilon_i}{m_i\chi_s}}\right)\exp(\chi) + \frac{\gamma}{1-\gamma}\sqrt{\frac{m_e\varepsilon_i}{m_i(\chi-\chi_s)}}, \tag{1}$$

where $\chi = e\varphi/kT_e$, normalized potential; $\chi_s = e\varphi_s/kT_e$, normalized sheath potential; $\xi = x/\lambda_D$, normalized distance; $\lambda_D = (\varepsilon_0 kT_e/ne^2)^{1/2}$, Debye length; $\varepsilon_i = v_{0i}^2 m_i/2kT_e$, normalized ion energy at the sheath edge.

The effective coefficient

$$\gamma = \frac{\gamma_{ee}}{\sin\,\alpha + \gamma_{ee}(1-\sin\,\alpha)} \tag{2}$$

is dependent on the effective electron emission coefficient γ_{ee} and the angle α between the magnetic field and the target surface. Here electrons are assumed to be emitted from the wall with thermal energies ($\ll kT_e$) . The effective electron emission coefficient

$$\gamma_{ee} = \frac{\gamma_e + \gamma_i + \gamma_t}{1 + \gamma_i + \gamma_t} \tag{3}$$

includes the electron-induced emission γ_e, the ion-induced one γ_i, and the photon-induced plus thermoelectron emission $\gamma_t = j/n_0(kT_e/m_i)^{1/2}$, where j is the emission flux due to photoemission and thermoelectron emission, and n_0 is plasma density.

The electric field E in the sheath at a distance x from the surface is determined assuming a boundary condition $E = 0$ in the plasma for $\chi = 0$:

$$\left(\frac{d\chi}{d\xi}\right)^2 = 4\varepsilon_i\left(\sqrt{1-\frac{\chi}{\varepsilon_i}} - 1\right) + 4\frac{\gamma}{1-\gamma}\sqrt{-\frac{m_e\varepsilon_i\chi_s}{m_i}}\left(\sqrt{1-\frac{\chi}{\chi_s}} - 1\right) + 2\left(1-\frac{\gamma}{1-\gamma}\sqrt{-\frac{m_e\varepsilon_i}{m_i\chi_s}}\right)(\exp(\chi) - 1). \tag{4}$$

This equation can be solved when the Bohm criterion

$$\varepsilon_i \geqslant \frac{1}{2} + \frac{\gamma}{1-\gamma}\sqrt{\frac{m_e}{m_i}}\left(-\frac{\varepsilon_i}{\chi_s}\right)^{3/2}\left(\frac{1}{2} - \chi_s\right) \tag{5}$$

is satisfied.

Using the fact that the ion flux must be balanced with the electron flux we have

$$\exp(\chi_s) = \sqrt{\frac{4\pi\varepsilon_i m_e}{m_i}\,\frac{1-\gamma+\gamma\,\sin\,\alpha}{1-\gamma-\gamma\sqrt{-\frac{m_e\varepsilon_i}{m_i\chi_s}}}}. \tag{6}$$

When $\alpha = \pi/2$, then $\gamma = \gamma_{ee}$ and Eqs. (4)–(6) become similar to those given by Hobbs and Wesson [3]. In order to obtain the self-consistent solution for Eq. (4) as a function of γ, we have determined ε_i and χ_s by an iterative process by setting a minimum of ε_i in Eq. (5) and solving Eq. (6). When the effective coefficient γ exceeds the critical value of 0.91, a virtual cathode is formed in front of the surface and the electric field there becomes zero. Such SCLC would set in during a local hot-spot formation on the divertor surface. It should be noted that the occurrence of SCLC is dependent both on γ_{ee} and α.

In the present work we have investigated how the effective secondary electron yield is affected by the potential distribution in the sheath for Be, C, Mo and W as the target materials. The results have been compared for two quite different conditions, for the ordinary regime ($\gamma = 0$) and for the SCLC ($\gamma = 0.91$) as shown in Fig. 1 for $\alpha = 10°$.

3. Data sets for secondary electron yield, reflection coefficient and energy distribution of the emitted electrons

For the calculation, basic data were required for secondary electron yield, reflection coefficient and energy distribution of emitted electrons. The secondary electron yield δ_e, was obtained with the Kollath's empirical formula $\delta_e(E_p)$ [4] by using δ_{max} and $E_{p,max}$ as given in Ref. [5], which also provided the energy distribution of the secondary electrons.

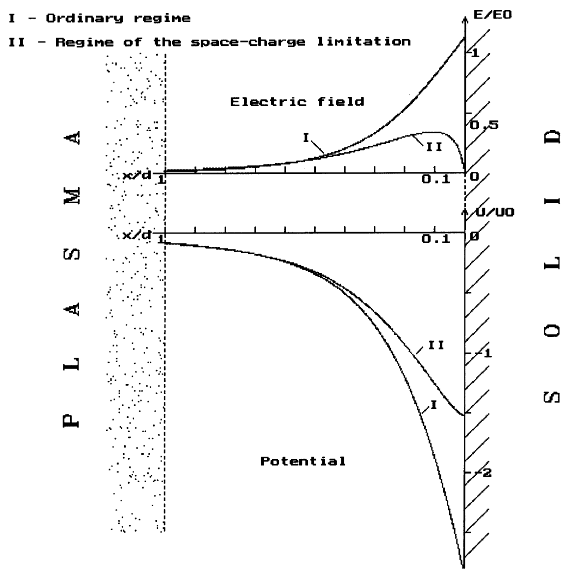

Fig. 1. Potential and electric field in the sheath for ordinary regime ($\gamma = 0$) and the space-charge limited regime ($\gamma = 0.91$). $E_0 = kT_e/e\lambda_D$, $U_0 = kT_e/e$.

As for the reflection coefficients η we used data given by Thomas [6] for W and C, Sternglass [7] for Mo and Bronshtein et al. [8] for Be. For energy and angular distributions of the reflected electrons we assumed simply a mirror reflection but the total number was reduced by the reflection coefficient η. When the reflected electrons are directly returned to the wall surface due to their gyration, they are expected to be reflected or to produce secondary electrons at the surface depending on their energy. One should note that the difference between high Z and low Z appears in both secondary electron and reflection yields. Because the penetration depth of primary electrons in high-Z materials is smaller than that in low-Z materials, not only the reflection coefficient but also the secondary electron yield is increased with higher Z.

4. Transport of emitted electrons in the sheath

The electron motions in the sheath were followed by solving a third-order Runge-Kutta method with an integration step chosen to ensure an error less than $10^{-4}\lambda_D$. Fig. 2 shows some traces of emitted electrons gyrating along magnetic field with a drift motion in perpendicular direction to the electric and magnetic fields. If the magnetic field is parallel to the surface and the gyroradius of electrons is much smaller than Debye length, all electrons are simply returned to the wall resulting in an effective secondary yield of zero. In the actual case, the magnetic field need not be parallel to the surface and the gyroradius of high energy electrons can be larger than a Debye length.

In the calculation we assumed a cos(θ) dependence of the ejected electrons in the present energy range (the angle θ is with respect to a surface normal). The angle between the magnetic field and a surface plane was set to $\alpha = 10°$, and the sheath thickness to $d = 5\lambda_D$ and $d = 10\lambda_D$.

5. Results and discussion

Fig. 3(a) shows how the potential and electric fields are influenced by values of γ. Calculations were made for 1 million primary electrons having primary energy E_p distributing from 100 eV to 10 keV. The number of electrons passing through the sheath per primary electrons was counted to determine the effective electron yield as a function of the primary energy. In Fig. 3(b) thus obtained effective electron yield δ_e is plotted against E_p. As seen in the figure, with increasing E_p, δ_e increases to a maximum at around 1 keV followed by a minimum at around 4 keV, and finally becomes energy independent above 4 keV. Above 4 keV, δ_e is also independent of the potential distribution in the sheath (γ).

Fig. 4 compares δ_e for W, Mo, C and Be in case of Te = 30 eV and $n_0 = 10^{18}$ m^{-3} between the ordinary regime ($\gamma = 0$) and the SCLC ($\gamma = 0.91$) one. Since for the latter case the electric field near the surface is much smaller than that for the ordinary regime, the number of electrons returned to the wall is larger. Consequently the effective electron yield is reduced about 1.7 times in the SCLC regime for all four materials compared with the ordinary regime. Such a large difference between the two regimes is mainly caused by the modified behavior of the

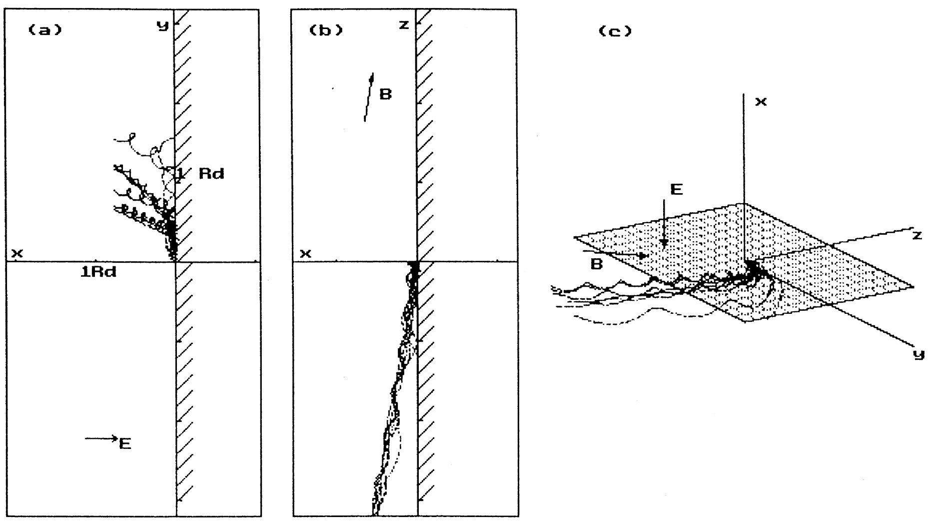

Fig. 2. Trajectories of secondary electrons, reflected and new produced electrons; (a) x–y plane; (b) x–z plane; (c) 3 dimensional view. Plasma temperature $T_e = 30$ eV, plasma density $n_0 = 10^{18}$ m^{-3}. Magnetic field strength $B = 2$ T and the magnetic inclination angle to surface is 10°; Debye length $R_d = 40$ μm.

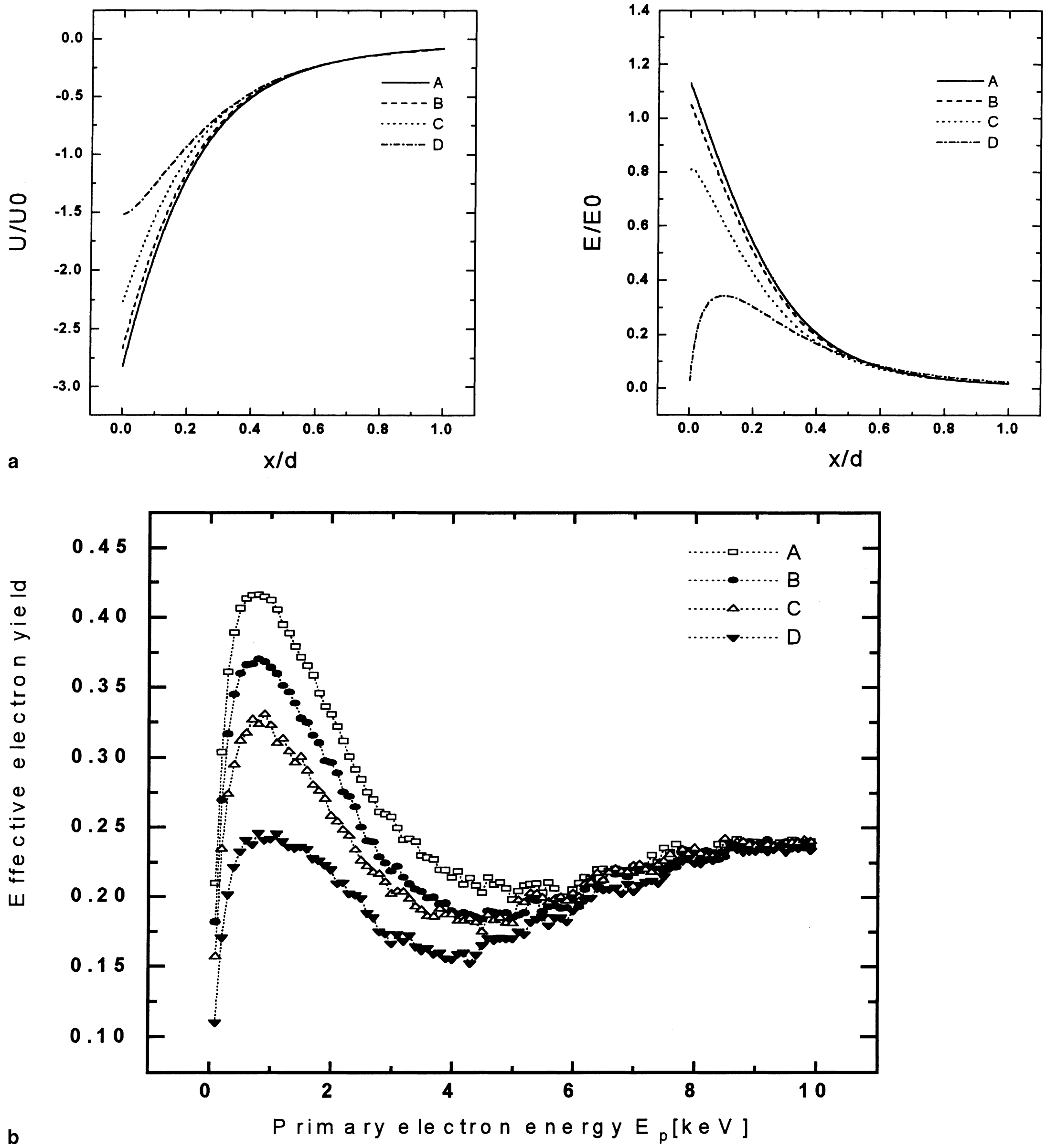

Fig. 3. (a). Variations of potential U and electric field E in the sheath with the effective coefficient γ; (A) $\gamma=0$, (B) $\gamma=0.5$, (C) $\gamma=0.8$, (D) $\gamma=0.91$. $E_0=kT_e/e\lambda_D$, $U_0=kT_e/e$, $\alpha=10°$. Here x/d is normalized distance, d is the sheath thickness. (b). Effective electron yield δ_e for W as a function of the primary electron energy E_p for different γ; (A) $\gamma=0$, (B) $\gamma=0.5$, (C) $\gamma=0.8$, (D) $\gamma=0.91$.

true secondary electrons which have low energy and directly return to the wall by gyration in the SCLC regime.

For high-Z materials (W, Mo), the contribution of the reflected electrons to the effective electron yield becomes appreciable with increasing primary electron energy as shown in Fig. 5, mainly because their reflection coefficient is much higher than low-Z materials (Be, C).

In Fig. 6 the effective secondary yields are compared between the two regimes for higher density case of $n_0 = 10^{19}$ m^{-3} (compare with Fig. 4). One can see a significant reduction of δ_e for the low energy region in the SCLC regime. Nevertheless the absolute number of the effective secondary electron yield is roughly two times or more larger in the higher density SCLC case than that in the low density case (compare with Fig. 4). This indicates that the space-charge limited condition is likely to occur in high plasma density case.

One should note that the difference in δ_e above 4 keV becomes smaller for all target materials and irrespective

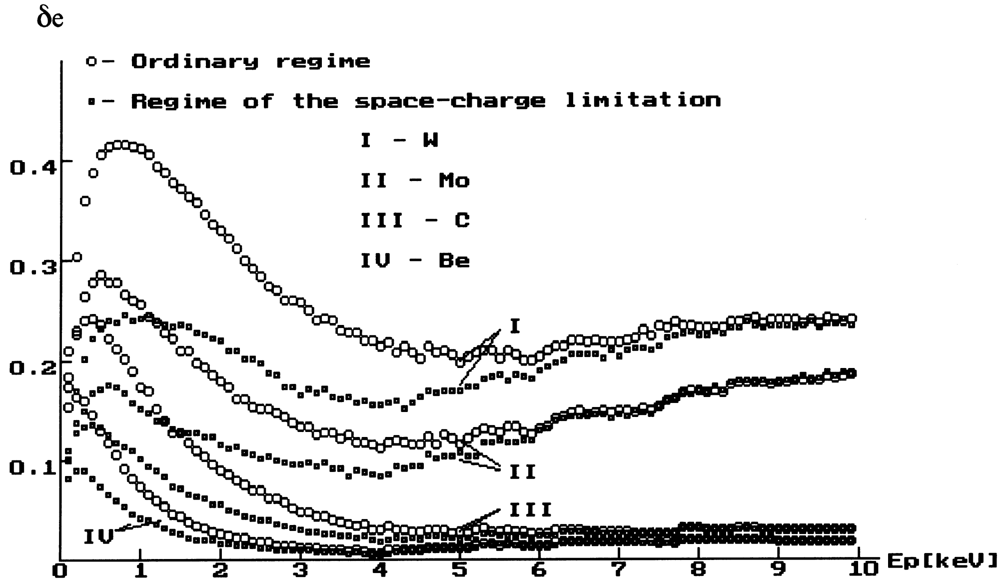

Fig. 4. Effective electron yield δ_e for W, Mo, C and Be against E_p. $T_e = 30$ eV, $n_0 = 10^{18}$ m^{-3}.

of plasma density (Figs. 4 and 6). That is because the gyro-radius of high-energy electrons is close to the sheath thickness and electrons easily escape from an oblique magnetic field. Even if the magnetic field was parallel to the surface, δ_e would not be zero owing to higher reflection.

Below a primary electron energy $E_p = 4$ keV the secondary electron yield is nearly the same for a sheath thickness $d = 10\lambda_D$ as for $d = 5\lambda_D$, as shown in Fig. 7. Above 4 keV, δ_e is smaller for $d = 10\lambda_D$. For $d = 5\lambda_D$ the secondary electron yield increases above 4 keV and for $d = 10\lambda_D$ above 16 keV, because the energy has to be

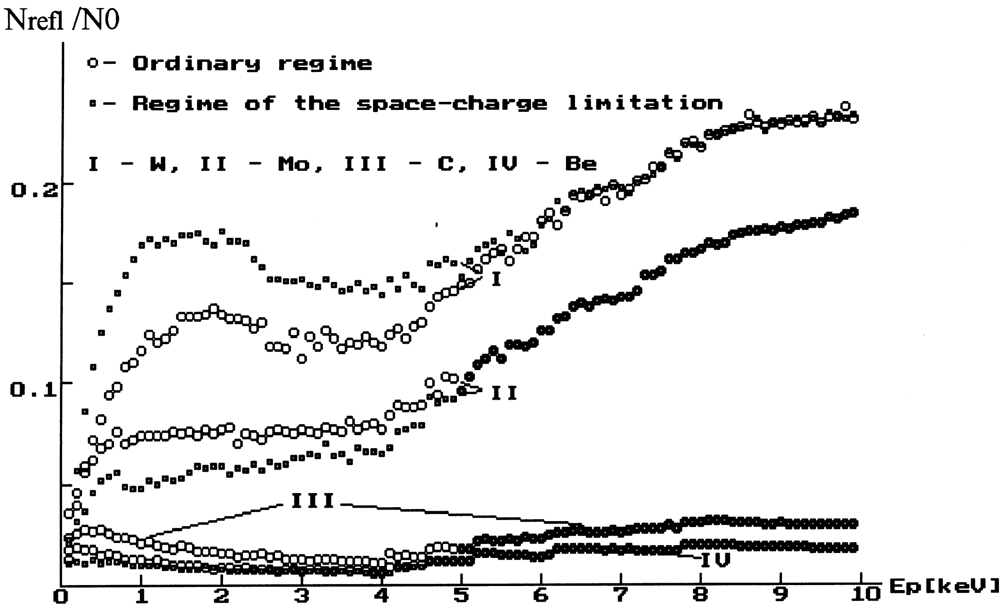

Fig. 5. Contribution of the reflected electrons on the effective electron yield as a function of E_p. $T_e = 30$ eV, $n_0 = 10^{18}$ m^{-3}.

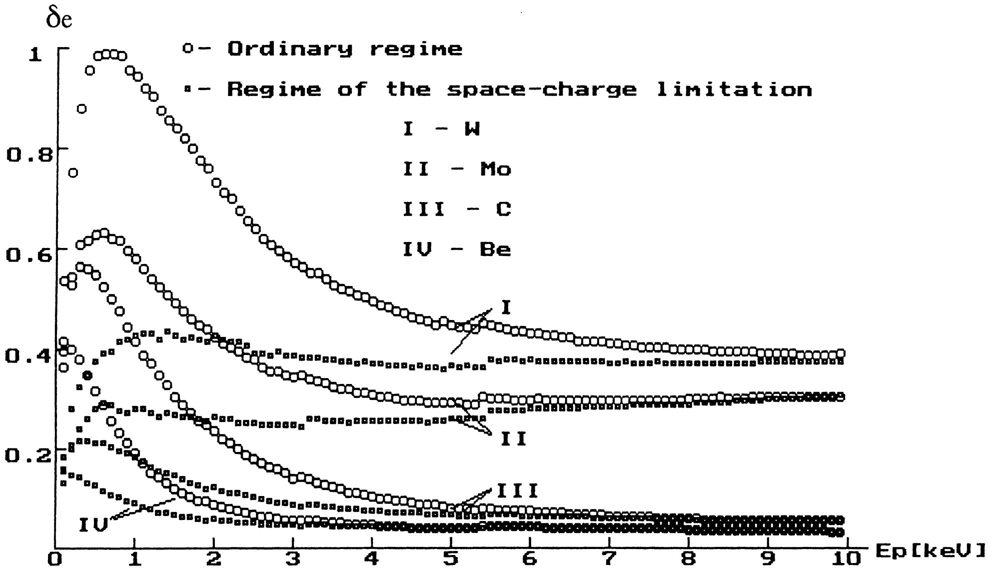

Fig. 6. Effective electron yield δ_e for W, Mo, C and Be against E_p. $T_e = 30$ eV, $n_0 = 10^{19}$ m^{-3}.

raised four times to increase gyration radius twice from $5\lambda_D$ to $10\lambda_D$.

Hence for low primary electron energy (below 4 keV) δ_e is independent of the sheath thickness, whereas for high primary electron energy δ_e is independent of the potential distribution in the sheath.

It should be mentioned that the electric field just in front of the surface dominates the effective secondary electron yield in the present simulation. This was confirmed by an additional calculation using the electric field $E(x) = E_0(x/d)^{1/3}$ for the Child–Langmuir space limitation [9] which has similar electric field to present SCLC regime for $x < \lambda_D$.

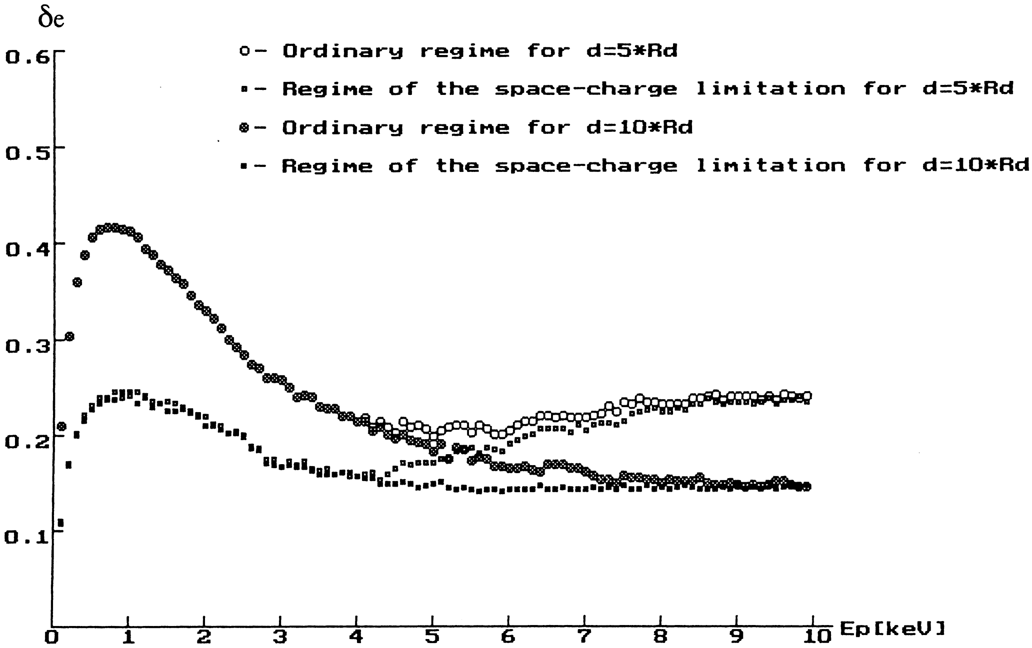

Fig. 7. Effective electron yield δ_e for W against E_p for the sheath thickness $d = 5\lambda_D$ and $d = 10\lambda_D$. $T_e = 30$ eV, $n_0 = 10^{18}$ m^{-3}.

6. Conclusions

For lower primary energy incidence, the effective secondary electron yield is substantially suppressed in the SCLC regime because of the significant reduction of the low energy secondary electrons (below 4 keV) owing to their direct return to the surface by the gyration. Accordingly the energy distribution of the emitted electrons is shifted to higher energy direction.

For higher primary energy incidence, the yield is dominated by the reflected electrons which have rather high energy and are less influenced on the oblique magnetic field. Therefore the yield becomes independent of the potential distribution in the sheath. In other words, the population of higher energy electron is not reduced and the number of electrons coming back to the plasma with energy above 4 keV would be enhanced. Such enhancement of high energy electron emission would increase the sheath potential resulting in the increase of both energy flux to the surface and sputtering yield. This effect seems very important for high-Z materials because of their high reflection coefficients.

Since the reflection coefficient of low-Z materials is generally small, the effect of the emitted electron does not seem important. However, because the secondary electron yield for Be and C increases above 4 keV, the enhancement of high energy electron emission could be observed for higher energy incidence. Nevertheless the absolute value δ_e for low-Z materials is much smaller than 1 and the appearance of the SCLC regime is unlikely.

In conclusion the effect of the secondary electron emission on the boundary plasma should be very important for high-Z materials but not for low-Z materials. In the present work we did not consider the influence of the high energy electron emission on the potential distribution in the sheath for simplicity. To develop more realistic self-consistent model it must be taken into account.

References

[1] T. Tanabe, Suppl. J. Nucl. Fusion 5 (1994) 129.
[2] N. Noda, V. Philipps, R. Neu, J. Nucl. Mater. 241–243 (1997) 227.
[3] G.D. Hobbs, J.A. Wesson, Plasma Phys. 9 (1967) 85.
[4] R. Kollath, in: S. Flugge (Ed.), Handbuch der Physik, vol. 21, Springer, Berlin, 1956, p. 232.
[5] J. Kawata, K. Nishimura, A. Harada, K. Ohya, Radiat. Effe. Def. Solids 142 (1996) 607.
[6] E.W. Thomas, Atomic and Plasma–materials Interaction Data for Fusion, vol. 1, 1991, p. 79.
[7] E.J. Sternglass, Phys. Rev. 95 (1954) 345.
[8] I.M. Bronshtein, R.B. Segal, Sov. Phys. – Solid State 1 (1959) 1142.
[9] I. Langmuir, Phys. Rev. 33 (1929) 954.